THE JOURNAL OF BIOLOGICAL CHEMISTRY VOL. 286, NO. 22, pp. 19958–19972, June 3, 2011

Neurotoxic 43-kDa TAR DNA-binding Protein (TDP-43) Triggers Mitochondrion-dependent Programmed Cell Death in Yeast*[S]

Received for publication, October 15, 2010, and in revised form, April 4, 2011 Published, JBC Papers in Press, April 6, 2011, DOI 10.1074/jbc.M110.194852

Ralf J. Braun[‡§], Cornelia Sommer[‡], Didac Carmona-Gutierrez[‡], Chamel M. Khoury[‡], Julia Ring[‡], Sabrina Büttner[‡], and Frank Madeo[‡1]

From the [‡]Institute of Molecular Biosciences, University of Graz, Humboldtstrasse 50, 8010 Graz, Austria and [§]Institute of Cell Biology, University of Bayreuth, 95440 Bayreuth, Germany

Pathological neuronal inclusions of the 43-kDa TAR DNA-binding protein (TDP-43) are implicated in dementia and motor neuron disorders; however, the molecular mechanisms of the underlying cell loss remain poorly understood. Here we used a yeast model to elucidate cell death mechanisms upon expression of human TDP-43. TDP-43-expressing cells displayed markedly increased markers of oxidative stress, apoptosis, and necrosis. Cytotoxicity was dose- and age-dependent and was potentiated upon expression of disease-associated variants. TDP-43 was localized in perimitochondrial aggregate-like foci, which correlated with cytotoxicity. Although the deleterious effects of TDP-43 were significantly decreased in cells lacking functional mitochondria, cell death depended neither on the mitochondrial cell death proteins apoptosis-inducing factor, endonuclease G, and cytochrome *c* nor on the activity of cell death proteases like the yeast caspase 1. In contrast, impairment of the respiratory chain attenuated the lethality upon TDP-43 expression with a stringent correlation between cytotoxicity and the degree of respiratory capacity or mitochondrial DNA stability. Consistently, an increase in the respiratory capacity of yeast resulted in enhanced TDP-43-triggered cytotoxicity, oxidative stress, and cell death markers. These data demonstrate that mitochondria and oxidative stress are important to TDP-43-triggered cell death in yeast and may suggest a similar role in human TDP-43 pathologies.

TDP-43[2] is an RNA-binding protein with pleiotropic functions, including pre-mRNA splicing, mRNA processing, and transport (1). Notably, TDP-43 is the major component of ubiquitin-positive inclusions in diseased brains in a subtype of frontotemporal lobar degeneration (FTLD-U) as well as in many cases of amyotrophic lateral sclerosis (ALS) (1). FTLD is the second most frequent form of presenile dementia after Alzheimer disease, whereas ALS constitutes the most common motor neuron disease (1). In patients suffering from both familial and sporadic ALS, mutations in the TDP-43-encoding *TARDBP* have been identified, supporting the notion that either the onset of toxicity due to TDP-43 aggregation or the loss of TDP-43 function triggers the neurological disorder (1, 2).

Diverse animal and cellular models, including mouse, rat, *Drosophila*, *Caenorhabditis elegans*, and mammalian cell culture, have been developed to dissect the molecular mechanisms governing TDP-43 proteinopathies (3–11). Transgenic animal models expressing wild-type or ALS-associated variants of TDP-43 display pathological, ubiquitinated protein aggregates in motor neurons with subsequent neuronal cell loss and progressive neurodegenerative phenotypes (6, 8, 9, 11, 12). Accordingly, expression of wild-type and disease-associated TDP-43 variants in mammalian cell cultures results in the formation of ubiquitin-positive cellular inclusions correlated with increased incidences of cell death (10). However, the molecular pathways of TDP-43-triggered neuronal cell loss remain to be identified.

Although the yeast *Saccharomyces cerevisiae* genome encodes no apparent ortholog of TDP-43 (13), heterologous expression of human TDP-43 results in phenotypes noticeably resembling TDP-43 pathology in higher model organisms and in diseased humans (13–15), including (i) the translocation of TDP-43 from the nucleus to the cytoplasm followed by the formation of cytoplasmic TDP-43 foci; (ii) the accumulation of TDP-43-specific inclusions, which are accelerated upon expression of disease-associated TDP-43 variants; (iii) the identification of the C terminus of TDP-43 to be essential for TDP-43 aggregation; (iv) the correlation of TDP-43 pathology with growth inhibition in yeast; and finally (v) the occurrence of plasma membrane permeabilization, which is highly suggestive of TDP-43-triggered cell death.

Yeast is a powerful, genetically tractable model organism for studying cell death (16–18). Morphological markers of apoptosis and necrosis have been discovered in yeast (19–21), and the

* This work was supported by German Research Foundation (Deutsche Forschungsgemeinschaft) Grant BR 3706/1-1 (a postdoctoral fellowship to R. J. B.); by Austrian Science Fund (Fonds zur Förderung der Wissenschaftlichen Forschung) Grants W1226-B18 DKplus Metabolic and Cardiovascular Disease (to C. S. and F. M.), S-9304-B05 (to C. M. K. and F. M.), "Lipotox" (to D. C.-G., C. M. K., and F. M.), and T-414-B09 (a Hertha-Firnberg Fellowship to S. B.); and by the European Commission Project Apoptosis Systems Biology Applied to Cancer and AIDS (APO-SYS) (to F. M.).

[S] The on-line version of this article (available at http://www.jbc.org) contains supplemental Tables S1 and S2 and Figs. S1–S11.

⌘ *Author's Choice*—Final version full access.

[1] To whom correspondence should be addressed. Tel.: +43-316-380-8878; Fax: +43-316-380-9898; E-mail: frank.madeo@uni-graz.at.

[2] The abbreviations used are: TDP-43, 43-kDa TAR DNA-binding protein; FTLD, frontotemporal lobar degeneration; FTLD-U, frontotemporal lobar degeneration with ubiquitin-positive inclusions; ALS, amyotrophic lateral sclerosis; AIF, apoptosis-inducing factor; mtDNA, mitochondrial DNA; DHE, dihydroethidium; PI, propidium iodide; SC, synthetic complete; mtmCherry, mitochondrion-targeted monomeric Cherry; ROS, reactive oxygen species; NDE, external NADH:ubiquinone oxidoreductase; NDI, internal NADH:ubiquinone oxidoreductase.

molecular mechanisms of cellular demise resemble those from higher organisms. The yeast genome encodes conserved regulators of cell death, including proteases like the yeast caspase 1 (Yca1p), the serine proteases Nma111p and Kex1p, the calpain-like cysteine protease Cpl1p, and the vacuolar aspartyl protease Pep4p (22–27), as well as mitochondrial proteins like apoptosis-inducing factor (Aif1p); Ndi1p, the yeast homolog of the AIF-homologous mitochondrion-associated inducer of death; and endonuclease G (Nuc1p) (23, 28–30). Consequently, yeast undergoes distinct cell death pathways, including cell death protease-dependent and -independent pathways (17), or distinct modes of death involving the mitochondrion (16). These pathways are mechanistically similar to those observed in neurodegenerative disorders, including critical contributions of oxidative stress, mitochondria, and aging (16, 31, 32). The high degree of conservation of lethal signals and processes throughout evolution from yeast to humans has prompted the use of yeast for studies of neurotoxic cell death (33–36).

In this study, we show that TDP-43 expression in yeast resulted in the formation of perinuclear and perimitochondrial aggregate-like foci and in the induction of oxidative stress and age-associated cytotoxicity culminating in apoptosis and necrosis. TDP-43-triggered cytotoxicity required mitochondrial functionality but depended neither on the release of the mitochondrial proteins Aif1p, Nuc1p, and cytochrome *c* nor on the activity of the cell death proteases Yca1p, Nma111p, Kex1p, Cpl1p, and Pep4p. Finally, we show that TDP-43-triggered cytotoxicity strictly correlated with respiratory capacity, mitochondrial DNA (mtDNA) stability, and respiratory chain activity, suggesting that oxidative stress, mitochondria, and respiration crucially influence neuronal death in TDP-43 pathologies.

EXPERIMENTAL PROCEDURES

Chemicals—Antimycin A, 4′,6-diamidino-2-phenylindole (DAPI), dihydroethidium (DHE), oligomycin, and propidium iodide (PI) were purchased from Sigma-Aldrich; myxothiazol was obtained from Chemos (Regenstauf, Germany); and Annexin V-FLUOS and reagents for "terminal deoxynucleotidyltransferase dUTP nick end labeling" (TUNEL) were purchased from Roche Applied Science (Mannheim, Germany).

Yeast Expression Plasmids—Yeast expression constructs used in this study are described in supplemental Table S1. TDP-43-WT, including the yeast Kozak sequence, was subcloned from pAG416Gal-TDP-43-WT via the SpeI and ClaI restriction sites into multiple cloning site 1 of a pESC vector using a PCR-based method. For this purpose, the following primers were designed: forward, 5′-GCG GTG ATC CCG GAT TCT AGA CTA GTA GGA G-3′ and reverse, 5′-TTA TAT CGA TCC CAT TCC CCA GCC AGA AGA CTT AGA ATC CAT G-3′.

Yeast Strains and Growth Conditions—Yeast strains used in this study are described in supplemental Table S2. All strains were grown, if not indicated otherwise, on synthetic complete (SC) medium lacking either uracil (SC-Ura) or both uracil and histidine (SC-Ura/-His) and containing 0.17% yeast nitrogen base (Difco, Otto Nordwald, Hamburg, Germany), 0.5% $(NH_4)_2SO_4$, a 30 mg/liter concentration of all amino acids (except 80 mg/liter histidine and 200 mg/liter leucine), and 30 mg/liter adenine with 2% glucose (SCD), 0.5% glucose and 1.5% galactose (SCDG), 2% galactose (SCG), or 2% glycerol (SCGly) as the carbon source. TDP-43 expression was under the control of galactose-regulated promoters (*Gal1*P for pAG416Gal and *Gal1–10*P for pESC, respectively). Transformed yeast strains were pregrown for 6 h in 100-ml flasks at 145 rpm at 28 °C in SCD-Ura or SCGly-Ura until an A_{600} of 0.4, and expression was then induced in 100-ml quadruple indented flasks by shifting to SCG-Ura and SCDG-Ura media for pAG416-URA and pESC-URA constructs, respectively. Co-expression of *NDI1* and TDP-43 was done analogously in SCDG-Ura/-His medium applying pBY011-*NDI1* with a *URA3* marker and pESC-TDP-43 constructs with a *HIS3* marker both under the control of the *Gal1–10* promoter.

For experiments in which chemical inhibitors of the respiratory chain were applied, cultures were at first grown in SCD-Ura in flasks as described above, then shifted to SCDG-Ura, and transferred into a 96-deep well format with 400 μl of growth medium/well. At least three wells were used per condition. Cultures in 96 deep wells were incubated at 28 °C with shaking for 15 h and then analyzed for clonogenicity.

Expression of yellow fluorescence protein (YFP)-tagged TDP-43 was done analogously in synthetic minimal medium (SMG-Ura) applying pRS416Gal-TDP-43 with a *URA3* marker under the control of the *Gal1* promoter. Co-expression of a mitochondrion-targeted monomeric Cherry (mtmCherry) and TDP-43 was performed analogously in SMG-Ura/-His applying pYX223-mtmCherry with a *HIS3* marker (37) and pESC-TDP-43 constructs with a *URA3* marker both under the control of the *Gal1–10* promoter.

Spot Dilution Assays—Yeast clones transformed with TDP-43 constructs or vector controls (pAG416Gal and pESC) were grown overnight in SCD-Ura medium. Cultures were normalized to an A_{600} of 1.0 in double distilled H_2O, serially diluted in double distilled H_2O, and spotted onto solid nutrient-containing media inducing (SCG-Ura) or repressing (SCD-Ura) expression of TDP-43. Plates were incubated for 2 days at 28 °C before analysis.

Clonogenic Assays for Measuring Cytotoxicity—Survival plating (clonogenicity) was performed as previously described (23, 28). Briefly, cell densities of yeast cultures expressing TDP-43 or vector controls were measured with an automated cell counter (CASY1, Roche Innovatis, Bielefeld, Germany). 500 cells were plated on selective glucose-containing agar plates (SCD-Ura or SCD-Ura/-His) on which expression is repressed. The colony-forming units (cfus), *i.e.* the number of colonies grown after 2 days of incubation at 28 °C, were determined using an automated colony counter (LemnaTech, Würselen, Germany).

Assays of Respiratory Capacity and mtDNA Content of Yeast Strains—For qualitative determination of respiratory deficiency, wild-type and knock-out strains were streaked out on YPD (4% glucose, 1% yeast extract, 2% Bacto peptone; Difco) and YPGly (3% glycerol, 1% yeast extract, 2% Bacto peptone). Plates were incubated at 28 °C for 3 days. Respiratory deficiency of the respective yeast strains was indicated by a growth deficiency on YPGly, which can only be used to support growth by respiration.

For quantitative clonogenic determination of respiratory capacity, wild-type and knock-out strains were grown over-

night in liquid YPD. 500 cells were plated on solid YPD and incubated at 28 °C for 2 days. The resulting colonies were then replica-plated onto solid nutrient-containing medium with glycerol as the sole carbon source. The number of cfus was determined after 2 days of incubation at 28 °C, and the proportions of colonies able to grow on YPGly were calculated. These values normalized to the respiratory capacity of the wild-type strain were taken as indicative of the respiratory capacity of the mutant strains.

Yeast knock-out strains were tested for the presence of intact inheritable mtDNA by mating them on YPD plates with the mating-type α strain deleted for *MIP1*, a nuclear gene encoding the catalytic subunit of the mtDNA polymerase necessary for maintenance of mtDNA. Although the Δ*mip1* strain lacks mtDNA, the diploid strain will receive wild-type alleles of mtDNA genes if the strains being examined contain intact mtDNA. After mating, cultures were selected for diploids by growth on SCD-Met/-Lys. Lack of growth on YPGly of the resulting diploid strains demonstrated the lack of mtDNA in a given knock-out strain.

Cultures of yeast knock-out strains were tested for the presence of extranuclear DNA, *i.e.* mtDNA nucleoids, by DAPI staining performed as described previously (38). Briefly, wild-type and knock-out strains were grown overnight in liquid YPD. 200 μl of cultures were harvested, fixed for 10 min in 100% methanol at RT, washed in PBS, stained with 1 μg/ml DAPI in PBS for 10 min at RT, and washed four times in PBS. Cells were resuspended in 50 μl of PBS. At least 150 stained yeast cells per strain and experiment were analyzed by fluorescence microscopy (see below) for the presence of extranuclear mtDNA nucleoids.

Measurement of Oxidative Stress and Plasma Membrane Permeabilization—Oxidative stress and plasma membrane permeabilization (morphological cell death) were measured by DHE and PI staining, respectively, as described previously (23, 28, 32, 39). Briefly, 5×10^6 cells/sample were pelleted in 96-well plates. Cell pellets in each well were resuspended in 250 μl of DHE or PI staining solution (2.5 μg/ml in PBS for DHE and 0.1 μg/ml in PBS for PI). After 10 min of incubation at RT, fluorescence was measured in the GENiosPro 96-well fluorescence plate reader (Tecan, Grödig, Austria) with the following settings: fluorescence, top; excitation, 515 nm; emission, 595 nm; gain, 45; number of reads, 6; integration time, 40 μs. Staining solution was used for blank measurements. Samples were measured in duplicate, and at least three samples were determined per strain and construct. For validating data on an individual cell basis, stained samples were measured by flow cytometry (BD FACSAria, BD Biosciences) with the following settings: filter sets, PE-A for DHE (excitation, 488/532 nm; emission, 578 nm) and PerCP-Cy5.5 for PI (excitation, 488/532 nm; emission, 695 nm); flow rate, 4. Results were analyzed with the BD FACSDiva software V5.0. 30,000 cells were evaluated per sample, and at least three samples were determined per conditions. Unstained samples were used as controls.

Determination of Morphological Markers of Apoptotic and Necrotic Cell Death—Annexin V/PI co-staining was performed as described previously (28). To determine the frequency of morphological phenotypes, cells were evaluated by flow cytometry (BD FACSAria) and BD FACSDiva software V5.0 with the following settings for Annexin V/PI: filter sets, FITC (excitation, 488 nm; emission, 519 nm) and PerCP-Cy5.5 (excitation, 488/532 nm; emission, 695 nm), spectral overlap PerCP-Cy5.5/FITC, 4.0; flow rate, 1. 30,000 cells were evaluated per sample, and at least three samples were determined per conditions. Unstained samples and PI only- and Annexin V only-stained samples were used as controls.

Fluorescence Microscopy—DHE-, PI-, and Annexin V/PI-stained cells were subjected to fluorescence microscopy (microscope: Zeiss Axioskop, Carl Zeiss, Vienna, Austria; digital camera: Visitron Systems Imaging Microscopy, Puchheim, Germany) with MetaMorph V6.2 software (Molecular Devices, Sunnyvale, CA). Stained yeast cells were mounted onto a slide without fixation. Images were obtained at RT using a Cy3 optical filter set for DHE and PI staining, an enhanced GFP optical filter set for Annexin V staining, and a differential interference contrast filter set for transmitted light images, applying a 40×/1.30 oil immersion objective (Carl Zeiss, Vienna, Austria). Images were attributed a pseudocolor and further processed using the IrfanView V4.25 software.

DAPI-stained cells were subjected to fluorescence microscopy (microscope: Zeiss Axioplan 2 Imaging, Carl Zeiss, Göttingen, Germany). Stained yeast cells were mounted onto a slide with fixation in low melting agarose (45 °C). The proportions of stained yeast cells lacking mtDNA nucleoids were obtained at RT using a DAPI optical filter set, applying a 100×/1.30 oil immersion objective (Carl Zeiss, Göttingen, Germany).

Yeast cells expressing YFP-tagged TDP-43 or YFP-tagged TDP-43 and mtmCherry or fixed cells expressing YFP-tagged TDP-43 co-stained with DAPI were subjected to confocal microscopy by using a TCS SP5 system (Leica Microsystems, Wetzlar, Germany) equipped with a 405 nm laser diode, 458–515 nm argon laser, and a 561 nm DPSS561 laser in combination with an inverted microscope equipped with a 63×/1.30 GLYC 21 °C UV glycerol objective. Images from cells expressing YFP-tagged TDP-43 were recorded successively with the following settings: excitation at 514 nm and emission at 529–579 nm for YFP; illumination at 514 nm for bright field. Images from cells expressing YFP-tagged TDP-43 and mtmCherry were recorded successively with the following settings: excitation at 488 nm and emission at 498–530 nm for YFP; excitation at 558 nm and emission at 650 nm for mtmCherry; illumination at 558 nm for bright field. Images from fixed cells expressing YFP-tagged-TDP-43 co-stained with DAPI were recorded successively with the following settings: excitation at 405 nm and emission at 433–507 nm for DAPI; excitation at 514 nm and emission at 529–579 nm for YFP; illumination at 514 nm for bright field. All images were further processed using the Leica Application Suite Advanced Fluorescence software V2.1.0 (Leica Microsystems).

Generation of Cell Extracts and Immunoblot Analyses—Yeast cell extracts were generated as described previously (40) with minor modifications. Briefly, 5×10^7 cells were pelleted by centrifugation. Cell pellets were resuspended in 100 μl of double distilled H_2O, and cell suspensions were mixed with 100 μl of 0.2 M NaOH. After incubation on ice for 15 min, cells were pelleted by centrifugation and resuspended in 100 μl of

Laemmli sample buffer (2% (w/v) SDS, 10% (v/v) glycerol, 2% (v/v) β-mercaptoethanol, 60 mM Tris-HCl, pH 6.8, bromphenol blue). After thorough mixing, cell suspensions were heated for 7 min at 97 °C, cooled down on ice, and frozen at −20 °C until use.

SDS-PAGE and immunoblot analyses were performed as described previously (41, 42) with minor modifications. Cell extracts were thawed at RT and centrifuged for 1 min at 16,000 × *g*. 12 μl of supernatant (equivalent to 6 × 10^6 cells) were used for separation on 12% SDS-polyacrylamide gels using a Mini Protean 3 SDS-PAGE separation apparatus (Bio-Rad). Protein transfer on PVDF membranes (Immobilon Transfer Membrane P, Millipore, Vienna, Austria) was performed in a wet blotting chamber (Hoefer, Holliston, MA). Membranes were blocked with 1% (w/v) nonfat milk in TBS for 1 h at RT or overnight at 4 °C. Incubation with the first antibody (diluted 1:1000 in TBS-T (1% (v/v) Tween 20) for rabbit polyclonal TDP-43 antibody (Abcam, Cambridge, UK) and diluted 1:40,000 in TBS-T for rabbit polyclonal RPL16 antibody) was performed for 1 h at RT or overnight at 4 °C. Membranes were washed with TBS-T three times for 10 min and then incubated for 1 h at RT with the respective secondary antibody coupled with horseradish peroxidase (goat anti-rabbit IgG (Sigma-Aldrich) diluted in 0.5% (w/v) nonfat milk in TBS-T). Membranes were washed with TBS-T three times for 10 min. Immunodetection was done using the enhanced chemiluminescence kit (ECL, GE Healthcare). Membranes were incubated for 3 min with ECL reagent. X-ray films (Curix Ultra UV-G, Agfa, Vienna, Austria) were exposed with chemiluminescence, and the developed films were digitalized using an imaging densitometer (PhosphorImager, GE Healthcare) with ImageQuant software (GE Healthcare). Images were further processed with IrfanView V4.25 software.

RESULTS

Human TDP-43 Forms Perimitochondrial Aggregate-like Foci in Yeast—Pathological TDP-43 aggregates are hallmarks of certain devastating proteinopathies, including ALS and FTLD-U (1). In this study, we initially aimed to validate whether TDP-43 aggregation can also be observed in yeast expressing human TDP-43 and its ALS-associated variant TDP-43-Q331K. In line with previous studies (13–15), we observed, upon expression of TDP-43 driven by a galactose-inducible promoter on a low copy plasmid (CEN6), distinct TDP-43 foci in both living and fixed yeast cells resembling TDP-43 aggregates (supplemental Fig. S1, A and B, respectively). Consistent with earlier reports (14, 15), expression of wild-type TDP-43 in yeast resulted in a dominant focus per cell, whereas expression of TDP-43-Q331K drove the formation of multiple foci (supplemental Fig. S1). In accordance with the finding of others (13, 14), we observed that TDP-43 foci are cytoplasmic with predominant perinuclear localization (supplemental Fig. S1*B*).

Mitochondrial dysfunction is a hallmark of multiple neurodegenerative disorders (43). Very recent studies described mitochondrial dysfunction and abnormal mitochondrial aggregation and localization in mammalian cell cultures and mouse models of TDP-43 proteinopathies (44–46). Therefore, we analyzed whether TDP-43 foci interact with mitochondria. Strikingly, the majority of TDP-43 foci were found in close vicinity of the tubular mitochondrial network (Fig. 1). Thus, our data confirm that TDP-43 aggregation occurs in yeast and further suggest a possible interplay between TDP-43 foci and mitochondria in yeast.

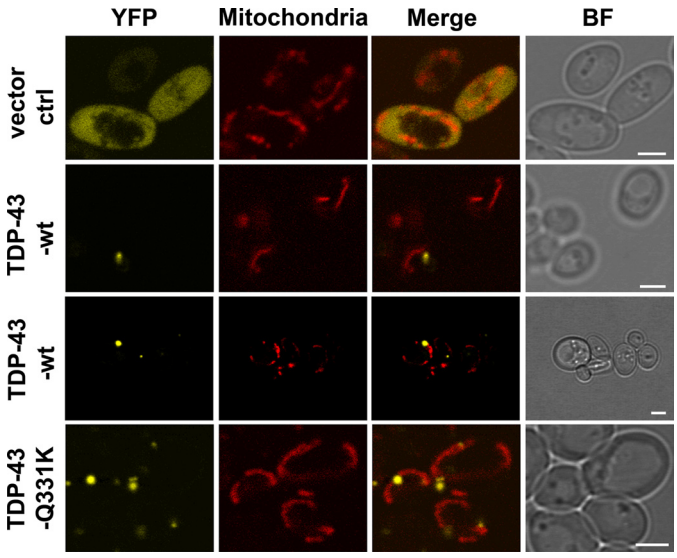

FIGURE 1. **Aggregate-like perimitochondrial foci upon expression of TDP-43 in yeast.** YFP-tagged human wild-type TDP-43 and ALS-associated TDP-43-Q331K were co-expressed overnight with red fluorescent mtmCherry from a low copy (CEN6) and a high copy (2μ) yeast expression plasmid, respectively, both under the control of a *GAL1* promoter in growth medium with galactose as the sole carbon source. Before microscopy, cultures were diluted in expression medium and incubated for 4 h to reach logarithmic growth phases. Images represent single layers applying confocal microscopy. *Scale bars*, 2.5 μm. Pseudocolor images are shown. *ctrl*, control; *BF*, bright field.

TDP-43 Expression Triggers Age-dependent Cytotoxicity and Oxidative Stress—In light of previous studies demonstrating loss of viability as a result of TDP-43 expression (6, 8, 9, 11, 12), we next examined whether human TDP-43 causes cytotoxicity in yeast. We initially applied serial spot dilution assays as a qualitative measurement of cytotoxicity. Expression of TDP-43 and TDP-43-Q331K under the control of a galactose-inducible promoter, using both low copy (CEN6) and high copy (2μ) plasmids, resulted in a markedly reduced growth (supplemental Fig. S2). These data demonstrate the deleterious effects of TDP-43 expression in yeast and are in line with data published previously (13–15).

Spot dilution assays neither allow a distinction between decreased growth rates and increased incidences of cell death nor measure effects in aging cultures (33). Therefore, we applied a survival assay wherein the proportion of viable cells able to form a colony (clonogenicity) on nutrient-containing solid medium is determined quantitatively (23, 28). Here, in contrast to spot dilution assays, the potential cytotoxic proteins are expressed in liquid cultures, and cells are thereafter plated on nutrient-containing medium repressing the expression of the respective protein. Changes in clonogenicity are then used to infer a measure of survival based on the rationale that only viable cells within the liquid culture retain the ability to form colonies on solid medium repressing expression.

For these clonogenic assays, expression of wild-type TDP-43 as well as that of the ALS-associated aggregation-prone variant TDP-43-Q331K was driven by a galactose-inducible promoter

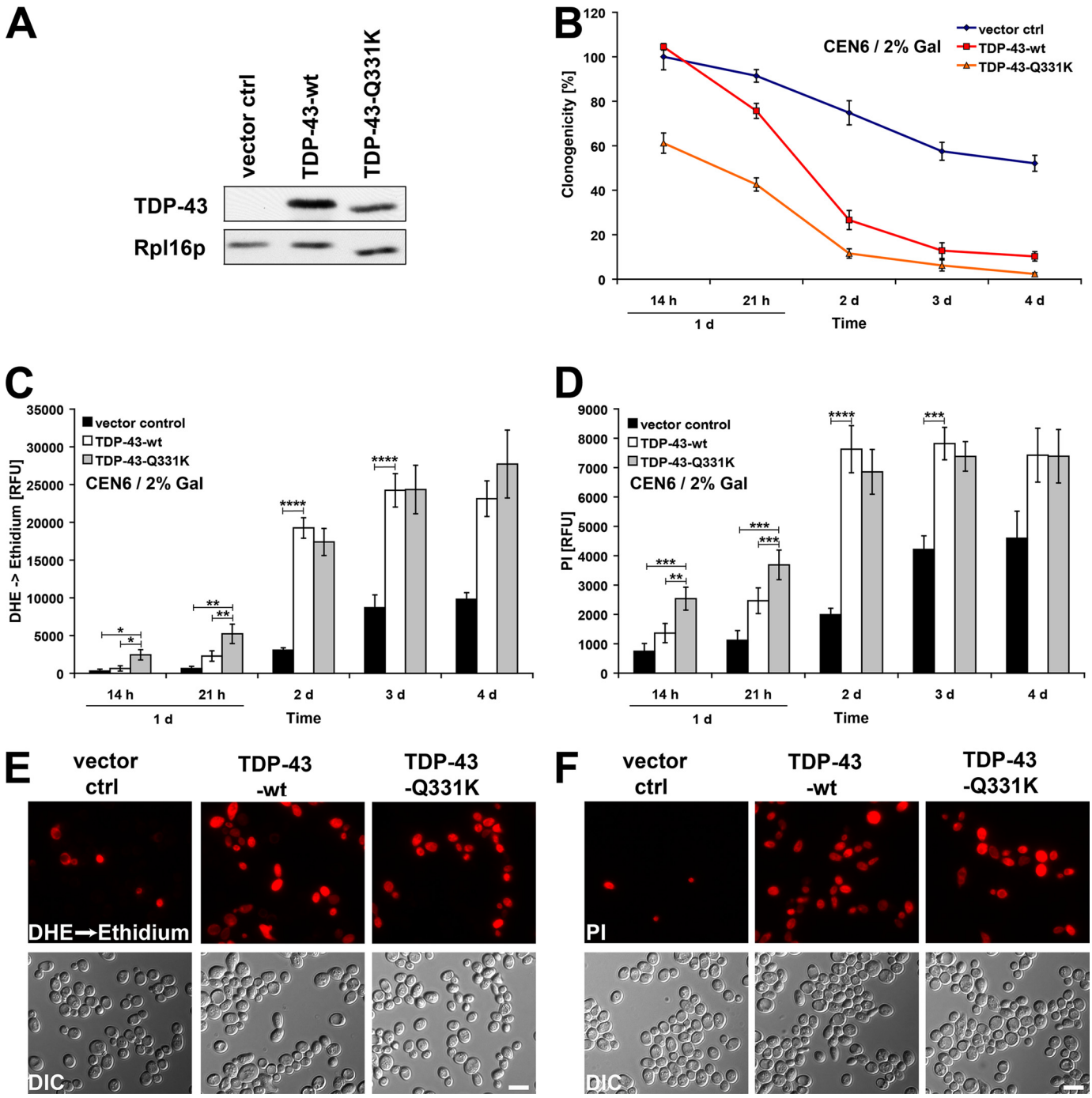

FIGURE 2. **Age-dependent TDP-43-triggered cytotoxicity in yeast.** Wild-type TDP-43 and TDP-43-Q331K (both untagged) were expressed from a low copy (CEN6) yeast expression plasmid under the control of a *GAL1* promoter in growth medium with galactose as the sole carbon source. *A*, immunoblot confirming TDP-43 expression. Rpl16p was used as loading control. *B*, yeast cells were evaluated for clonogenicity at the indicated time points after induction of expression. Data represent mean values of at least five independent experiments. *Error bars* represent S.E. *C* and *D*, oxidative stress levels (DHE staining) and incidences of membrane permeabilization (PI staining) were measured using a fluorescence plate reader at the indicated time points after induction of TDP-43 expression. Data represent mean values of at least three independent experiments. *Error bars* represent S.E. *, $p < 0.05$; **, $p < 0.01$; ***, $p < 0.001$; ****, $p < 0.0001$ (*t* test, paired). *E* and *F*, DHE- and PI-stained cells from *C* and *D* collected at day 2 after induction of TDP-43 expression were analyzed by fluorescence microscopy. Please note that plasma membrane permeabilization upon TDP-43 expression was already reported (13). *Scale bars*, 5 μm. Pseudocolor images are shown. *ctrl*, control; *RFU*, relative fluorescence units; *d*, day(s).

on a low copy plasmid (CEN6) (Fig. 2*A*). Expression of wild-type TDP-43 did not lead to a marked decrease in clonogenicity at day 1 (14 h) after induction (Fig. 2*B*) in contrast to a high copy plasmid (2μ), which achieved a nearly 80% decrease in clonogenicity at the same time point (supplemental Fig. S3*A*). However, upon further chronological aging of the yeast cultures, clonogenicity upon expression of wild-type TDP-43 was significantly decreased, reaching very low levels at days 3 and 4 of induction (Fig. 2*B*). Interestingly, the expression of the ALS-associated variant TDP-43-Q331K resulted in an accelerated and more severe decrease in clonogenicity when compared with wild-type TDP-43 (Fig. 2*B*).

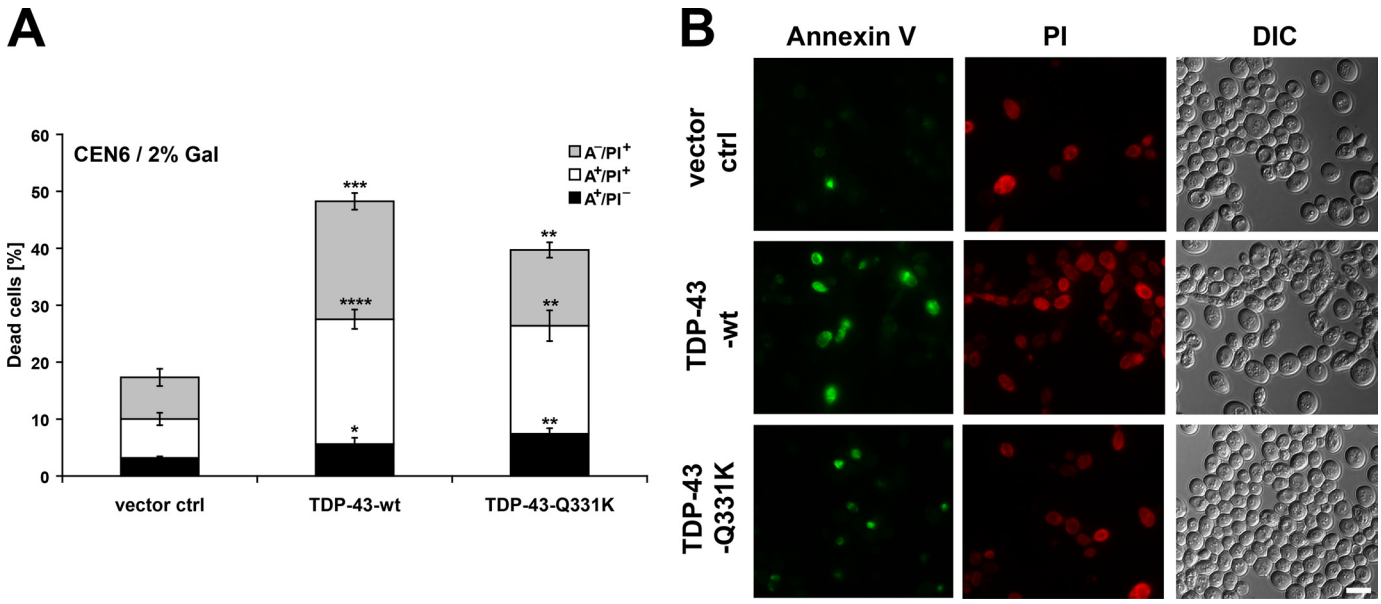

FIGURE 3. **Apoptotic and necrotic cell death in TDP-43-expressing yeast cells.** TDP-43 was expressed from the low copy (CEN6) expression plasmid as in Fig. 2. Two days after inducing TDP-43 expression, yeast cells were evaluated for morphological markers of cell death. Annexin V (*A*)$^+$/PI$^-$ and Annexin V$^-$/PI$^+$ yeast cells are referred to as (early) apoptotic and necrotic, respectively. Annexin V$^+$/PI$^+$ yeast cells are referred to as late apoptotic and secondary necrotic. *A*, quantitative measurement of cell death using FACS analysis. Data represent mean values of five independent experiments. *Error bars* represent S.E. *p* values were determined with a *t* test by comparing vector controls with TDP-43-WT and TDP-43-Q331K, respectively. *, $p < 0.05$; **, $p < 0.01$; ***, $p < 0.001$; ****, $p < 0.0001$. *B*, Annexin V/PI-stained cells from *A* analyzed by fluorescence microscopy. *Scale bar*, 5 μm. Pseudocolor images are shown. *ctrl*, control; *DIC*, differential interference contrast.

We next examined whether our clonogenicity data correlated with the presence of morphological cell death markers, specifically oxidative stress and plasma membrane permeabilization. The former can be detected by the conversion of the ROS-sensitive stain DHE to fluorescent ethidium, whereas the latter is measured through the cellular incorporation of the fluorescent "vital dye" PI (23, 28). Accordingly, both ROS accumulation and the relative levels of PI-positive cells were significantly increased in cells expressing wild-type TDP-43 with the most severe effects observed after 2 days of induction (Fig. 2, *C* and *E* and *D* and *F*, respectively). Consistent with the clonogenicity data, ROS accumulation and plasma membrane permeabilization occurred at significantly earlier time points upon expression of TDP-43-Q331K (day 1, 14 and 21 h) when compared with cells expressing wild-type TDP-43 (Fig. 2, *C* and *D*). These data demonstrate that TDP-43 expression results in decreased cell survival (increased cytotoxicity), elevations in oxidative stress, and enhanced plasma membrane permeabilization. Furthermore, we found these effects to be dose-dependent, exacerbated upon chronological aging, and potentiated in cells expressing the ALS-associated variant TDP-43-Q331K.

TDP-43-triggered Cell Death Displays Markers of Apoptosis and Necrosis—Distinct subroutines of programmed cell death, such as apoptosis and necrosis, have been observed in yeast and are highly similar to those occurring in mammalian cells with respect to a number of features (18). To determine the mode of cell death triggered by the low copy expression of TDP-43, we performed Annexin V/PI double staining. Annexin V labels externalized phosphatidylserine that appears on the surface of apoptotic cells, whereas PI, as mentioned before, is a vital dye that stains cells that have lost plasma membrane integrity during necrotic cell death. Therefore, Annexin V-positive and PI-positive cells are considered to be apoptotic and necrotic, respectively. Co-stained populations are interpreted to be secondary necrotic cells in which apoptosis was initiated but ultimately succumbed to necrotic subroutines. Applying these staining techniques, we observed increased levels of apoptotic (Annexin V$^+$/PI$^-$ and Annexin V$^+$/PI$^+$) and necrotic death (Annexin V$^-$/PI$^+$) after 2 days of induction of either wild-type or ALS-associated TDP-43-Q331K when compared with empty vector controls (Fig. 3). Results from TUNEL analysis, detecting apoptotic fragmentation of nuclear DNA, confirmed the induction of apoptosis upon expression of TDP-43 (data not shown). Thus, TDP-43 expression in yeast triggers both apoptotic and necrotic cell death.

TDP-43-triggered Cytotoxicity Is Suppressed in mtDNA-deficient Yeast—Both apoptotic and necrotic cell death scenarios in yeast rely extensively on mitochondrial events and/or the activation of proteases that execute the final stages of cell death (16, 18). To determine whether mitochondrial processes and/or cell death proteases mediate TDP-43-triggered cytotoxicity, we expressed TDP-43 in yeast strains deleted for either mtDNA (ρ^0 strains) or individual yeast cell death proteases (Fig. 4 and supplemental Fig. S6). ρ^0 strains are unable to perform respiratory metabolism and thus do not efficiently grow when forced to use galactose as the sole carbon source. Thus, to induce expression of TDP-43 in mtDNA-deleted ρ^0 and mtDNA-containing ρ^+ strains, we used previously developed conditions in which 0.5% glucose is added to 1.5% galactose to reach the conventional 2.0% final concentration of carbon source (47). On the one hand, this intervention led to a decreased expression level of TDP-43 in ρ^+ strains when compared with ρ^+ strains grown in liquid medium containing galactose as the sole carbon source (supplemental Fig. S3*B*) and consequently to a

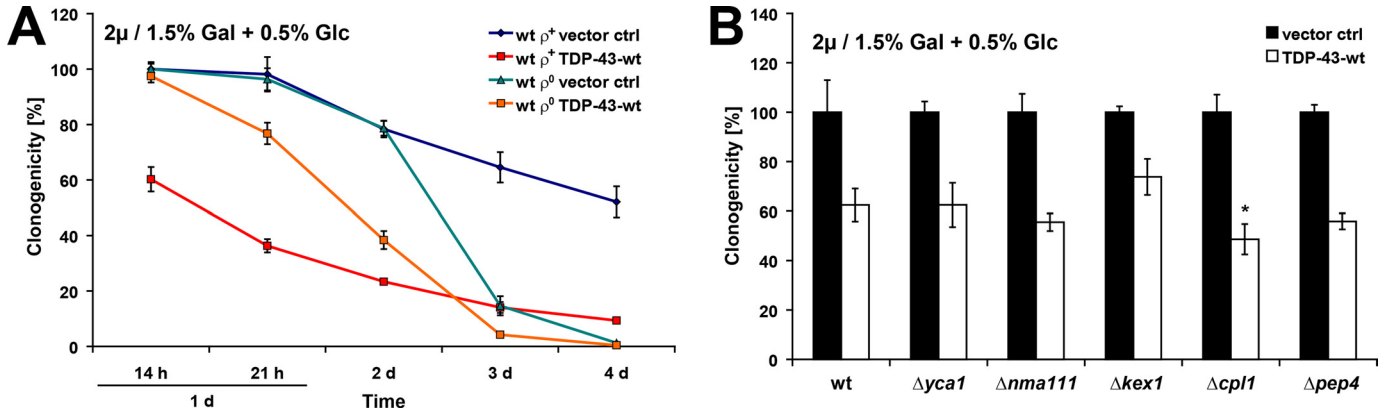

FIGURE 4. **Depletion from mtDNA relieves TDP-43-triggered cytotoxicity.** *A*, TDP-43 was expressed from a high copy (2μ) yeast expression plasmid under the control of a *GAL10* promoter in wild-type ρ^+ and mtDNA-depleted ρ^0 strains in nutrient-containing growth medium with glucose for fermentative growth and galactose for the induction of TDP-43 expression. Yeast cultures were evaluated for clonogenicity at the indicated time points. Data represent mean values of at least three independent experiments. *Error bars* represent S.E. *B*, TDP-43 was expressed as described in *A* in wild-type and knock-out strains deleted for genes encoding yeast cell death proteases for 14 h and evaluated for clonogenicity. The mean value of the cfus of yeast cells expressing vector controls was set to 100%. Data represent mean values of at least four independent experiments. *Error bars* represent S.E. *p* values were determined with a *t* test by comparing relative clonogenicity of TDP-43-WT in the wild-type strain *versus* knock-out strains. *, $p < 0.05$. *ctrl*, control; *Glc*, glucose; *d*, day(s).

decreased level of TDP-43-triggered cytotoxicity (compare ρ^+ strains in supplemental Fig. S3*A* and Fig. 4*A*). On the other hand, the intervention reduced the severity of the switch from glucose to galactose catabolism and allowed for expression of TDP-43 in both ρ^0 and ρ^+ strains (data not shown). After 14 h of growth under these conditions, ρ^0 cells displayed a complete abrogation of TDP-43-triggered cell death when compared with ρ^+ cells (Fig. 4*A*). Interestingly, increasing the duration of induction resulted in cytotoxicity of TDP-43-expressing ρ^0 strains albeit to a markedly lower extent as compared with ρ^+ strains, indicating a partial dependence on mitochondria for TDP-43-triggered lethality (Fig. 4*A*). At later time points (starting between days 2 and 3), ρ^0 strains (expressing both vector controls and TDP-43) demonstrated a dramatic decrease in clonogenicity consistent with previous reports on the considerably decreased chronological life span of these strains (47).

We next analyzed ρ^+ and ρ^0 strains for levels of oxidative stress and plasma membrane permeabilization upon TDP-43 expression. Because of the absence of the ROS-generating respiratory chain, ρ^0 strains exhibited reduced levels of both oxidative stress and plasma membrane permeabilization when compared with the ρ^+ strains at early time points (day 1, 21 h and day 2) (supplemental Fig. S6, *A* and *B*). At later time points coinciding with the period during which the clonogenicity of ρ^0 strains was dramatically reduced, both oxidative stress and plasma membrane permeabilization in ρ^0 strains were markedly elevated when compared with the ρ^+ strains (supplemental Fig. S6, *A* and *B* and see Fig. 4*A*). Notably, TDP-43 expression in neither the ρ^+ nor the ρ^0 strains resulted in a significant increase in oxidative stress levels or membrane permeabilization after culture in semifermentative growth conditions (galactose/glucose medium) (supplemental Fig. S6, *A* and *B*). A slight increase of oxidative stress levels and membrane permeabilization occurred only at later time points (days 3 and 4 for DHE staining and days 2–4 for PI staining) in the ρ^+ strains expressing TDP-43 (supplemental Fig. S6, *A* and *B*).

To validate the clonogenicity data obtained using the wild-type ρ^0 strain, we expressed TDP-43 in yeast strains deleted for nuclear genes encoding mitochondrial proteins that are necessary for maintenance of mtDNA in yeast (38). For this, we chose Δ*mgm1*, Δ*oxa1*, and Δ*atp4* strains that are deleted for genes involved in mitochondrial genome maintenance, mitochondrial protein import machinery, and mitochondrial ATP synthesis, respectively. Similar to the wild-type ρ^0 strain, these strains are deficient in respiration (confirmed by their inability to utilize glycerol as the sole carbon source (supplemental Figs. S4 and S6*D*)) and lack mtDNA (confirmed by (i) their inability to complement the ρ^0 phenotype of the Δ*mip1* strain deleted for the mtDNA polymerase (supplemental Fig. S5) and (ii) the absence of mtDNA nucleoids in these strains analyzed by DAPI staining (supplemental Fig. S6*E*)). TDP-43 expression in Δ*mgm1*, Δ*oxa1*, and Δ*atp4* strains resulted in a significant suppression of clonogenic cytotoxicity when compared with the wild-type strain (supplemental Fig. S6*C*). Collectively, these findings indicate that the presence of mtDNA and mitochondrial function play an active role in promoting TDP-43-triggered cytotoxicity and cell death.

Applying the same semifermentative growth conditions, we expressed TDP-43 in strains deleted for specific yeast cell death proteases, namely Yca1p, the serine proteases Nma111p and Kex1p, the calpain-like cysteine protease Cpl1p, and the vacuolar aspartyl protease Pep4p. Upon TDP-43 expression ("TDP-43 stress"), yeast strains deleted for *YCA1*, *NMA111*, and *PEP4* demonstrated a loss of clonogenicity comparable with that observed in the wild-type strain (Fig. 4*B*). Similar results were obtained when we applied acetate and tunicamycin stress (supplemental Fig. S7). Thus, upon semifermentative growth conditions, these cell death proteases are not involved in the execution of cell death, regardless of whether cell death was induced by TDP-43 expression or by acetate or tunicamycin stress.

Upon TDP-43 stress, the yeast strain deleted for *KEX1* demonstrated a mild but insignificant reduction in loss of clonogenicity as compared with the wild-type strain (Fig. 4*B*). Although acetate stress led to a similar loss of clonogenicity as compared with the wild-type strain (supplemental Fig. S7*A*), tunicamycin treatment resulted in a significant increase in clonogenicity

(supplemental Fig. S7*B*). Thus, Kex1p mediates cell death upon tunicamycin stress but does not play significant roles in the execution of TDP-43- (or acetate)-triggered cell death.

CPL1-deleted cells demonstrated a moderate but significantly increased loss of clonogenicity upon TDP-43 stress (Fig. 4*B*). Similar results were obtained upon acetate stress (supplemental Fig. S7*A*), whereas upon tunicamycin stress, loss of Cpl1p did not have any significant effect on the loss of clonogenicity as compared with wild-type strain (supplemental Fig. S7*B*). Therefore, upon TDP-43 (or acetate) stress, Cpl1p appears to play a protective role during cell death. Taken together, our data indicate that the cell death proteases tested herein in contrast to mitochondria are not essential cell death executors during TDP-43-triggered cell death.

Disrupting the Respiratory Chain Relieves TDP-43-triggered Cytotoxicity—Distinct cell death pathways are mediated by the cytoplasmic release of specific mitochondrial proteins. We thus sought to determine whether the effects of TDP-43 expression in yeast are dependent on the known mitochondrial programmed cell death regulators Aif1p, Nuc1p, and the two isoforms of cytochrome *c*, Cyc1p and Cyc7p (28, 29, 48). Deletion of neither *AIF1*, *NUC1*, *CYC1*, nor *CYC7* relieved TDP-43-triggered clonogenic cytotoxicity (supplemental Fig. S8). Thus, under the applied growth conditions, TDP-43-triggered cytotoxicity is independent of specific mitochondrial permeabilization for these proteins.

In addition to the release of mitochondrial prodeath proteins, impaired or inefficient mitochondrial respiratory chain activity can lead to cell death often concomitantly with the accumulation of ROS (16). NADH:ubiquinone oxidoreductases (NDI/NDE) and complex II supply electrons to the mitochondrial respiratory chain, and complexes III and IV mediate the flow of these electrons through the chain to establish the mitochondrial membrane potential and the proton gradient that is ultimately used by complex V for ATP synthesis (supplemental Fig. S9). To test the contribution of these elements to TDP-43-triggered lethality, we systematically analyzed the effects of TDP-43 expression in yeast strains deleted individually for NDI/NDE and components of complexes II–V. These strains exhibited various levels of respiratory deficiency and mtDNA content but unlike ρ^0 strains retained the ability to propagate intact mtDNA (Fig. 5 and supplemental Figs. S4, S5, and S10). Respiratory deficiency was determined both qualitatively by analyzing the ability of the yeast strains to grow on nutrient-containing solid medium with the obligatory respiratory carbon source glycerol (supplemental Fig. S4) and quantitatively by determining the proportions of yeast clones from the respective yeast strains that are able to adapt from fermentative (glucose) to obligatory respiratory growth conditions (glycerol; clonogenic respiratory capacity) (Fig. 5, *panel 2*, and supplemental Fig. S10, *panel 2*). The content of mtDNA was demonstrated by measuring the proportion of cells within a yeast culture lacking mtDNA nucleoids by DAPI staining (Fig. 5, *panel 4*, and supplemental Fig. S10, *panel 4*), and the ability of the strains to propagate intact mtDNA was confirmed by their ability to complement the ρ^0 phenotype of the Δ*mip1* strain deleted for the mtDNA polymerase (supplemental Fig. S5).

Although deletion of *NDE1* or *NDE2* did not significantly relieve TDP-43-triggered cytotoxicity, a mild but significant decrease in cytotoxicity was observed in the absence of the internal NADH:ubiquinone oxidoreductase *NDI1* (supplemental Fig. S10*A*, *panel 1*). Also, TDP-43-triggered cytotoxicity was markedly relieved in strains lacking essential components of complex II (*e.g.* the succinate dehydrogenase subunits Sdh1p and Sdh2p) (supplemental Fig. S10*B*, *panel 1*), complex III (*e.g.* the core subunit Cor1p and the Rieske iron-sulfur protein Rip1p, respectively) (Fig. 5*A*, *panel 1*), complex IV (*e.g.* the cytochrome *c* oxidase subunits Cox5ap and Cox9p) (Fig. 5*B*, *panel 1*), and complex V (*e.g.* the ATP synthetase subunits Atp10p and Atp18p) (Fig. 5*C*, *panel 1*). Notably, we observed that the extent to which TDP-43-triggered cytotoxicity was suppressed by a given genetic intervention strongly correlated with a reduction in respiratory capacity (Fig. 5, *panel 3*, and supplemental Fig. S10, *panel 3*). For instance, the deletion of the complex III subunits encoded by *QCR8* and *COQ4* relieved TDP-43-triggered cytotoxicity as well as respiratory capacity to lower extents than deletions in those encoded by *COR1* and *RIP1* (Fig. 5*A*, *panels 1–3*). Specifically, the coefficient of determination, R^2, ranged from 0.69 for NDI/NDE to 0.96 for complex III, meaning that 69–96% of the observed variation in TDP-43-triggered cytotoxicity was a consequence of the altered respiratory capacity in knock-out strains.

We observed that the yeast strains with reduced respiratory capacity demonstrated an increased number of cells lacking mtDNA (Fig. 5, compare *panels 2* and *4*, and supplemental Fig. S10, compare *panels 2* and *4*), suggesting a decreased mtDNA stability in these strains. Therefore, we analyzed whether the extent to which TDP-43-triggered cytotoxicity was suppressed by a given genetic intervention also correlated with the increase in the number of cells depleted from mtDNA in these strains (Fig. 5, *panel 5*, and supplemental Fig. S10, *panel 5*). In fact, we observed an increased correlation between the relief of TDP-43-triggered cytotoxicity and the reduced mtDNA content in the strains for complexes II, III, IV, and V (Fig. 5, *panel 5*, and supplemental Fig. S10*B*, *panel 5*). Specifically, the coefficient of determination, R^2, ranged from 0.77 for complex II to 0.84 for complex V, 0.98 for complex III, and 0.99 for complex IV, meaning that 77–99% of the observed variation in TDP-43-triggered cytotoxicity was a consequence of the altered mtDNA content in knock-out strains. For NDI/NDE, we could not observe any correlation between the relief of TDP-43-triggered cytotoxicity and the mtDNA content (supplemental Fig. S10*A*), suggesting mtDNA-independent effects.

To test whether the electron flux through the respiratory chain is necessary for TDP-43-triggered cytotoxicity, we cultured TDP-43-expressing cells in the presence of specific inhibitors of complex III (antimycin A or myxothiazol) and of the mitochondrial ATP synthetase complex (oligomycin) (supplemental Fig. S9). Antimycin A and myxothiazol significantly decreased the clonogenicity of the cultures expressing vector controls but were not able to further increase TDP-43-triggered cytotoxicity (Fig. 6, *A* and *B*). A similar, albeit slightly lower, effect was observed for cultures of TDP-43-expressing cells treated with oligomycin (Fig. 6*C*). These findings clearly indicate that the toxicity caused by pharmacological electron

transport inhibitors is not synergistic to TDP-43-triggered cytotoxicity and suggest that TDP-43 needs mitochondrial energization for efficient cell killing.

Forced Enhancement of Respiration Increases TDP-43-triggered Clonogenic Cytotoxicity—Decreased respiration by inhibition of the respiratory chain upon deletion of mtDNA or

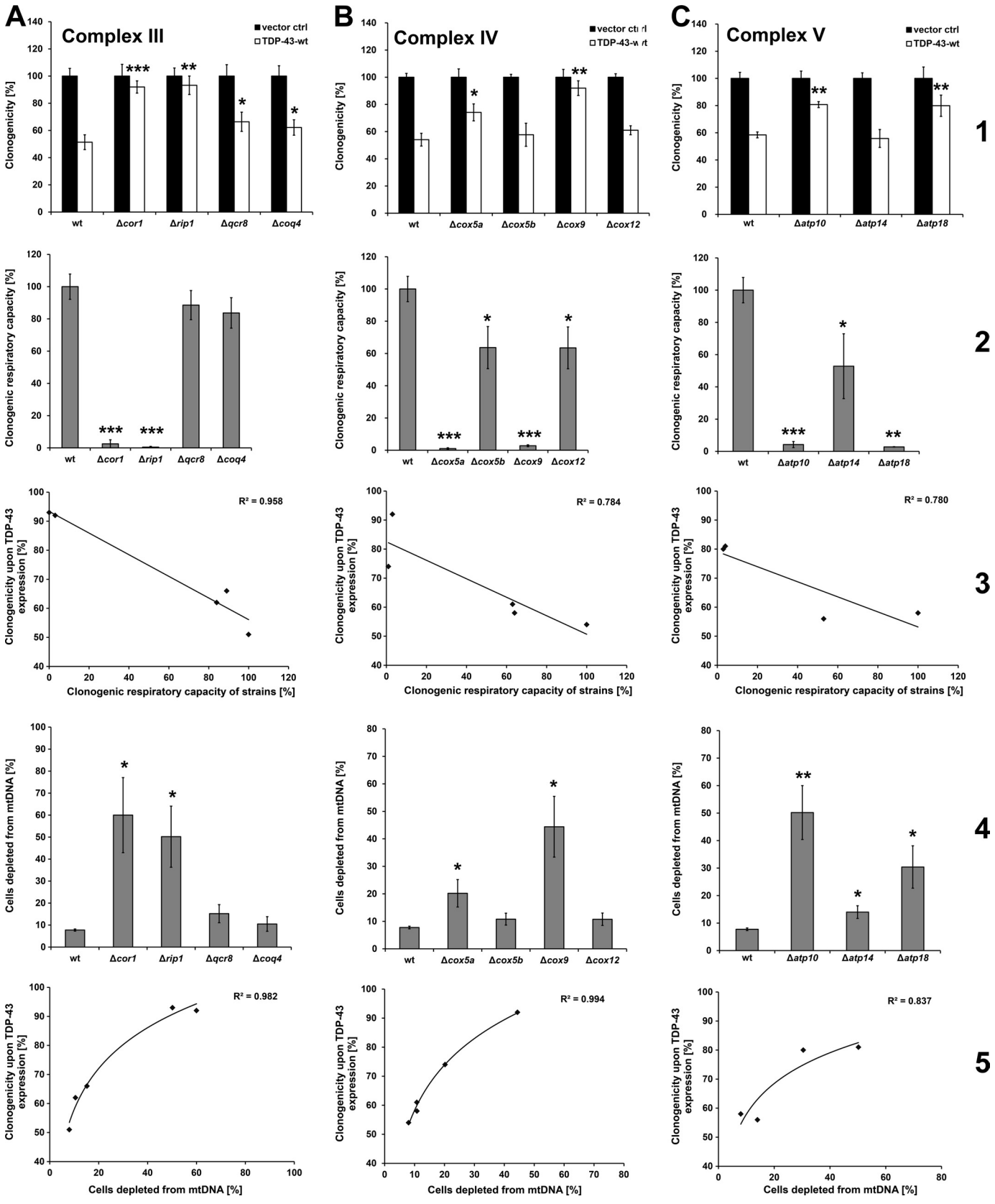

upon disruption of essential components of the respiratory chain complexes relieved TDP-43-triggered cytotoxicity (Figs. 4 and 5 and supplemental Figs. S6 and S10). However, decreased respiration and elevated fermentation are known to increase (rather than decrease) cell death, consequently resulting in a reduced chronological life span in yeast (49, 50). We first adapted our wild-type yeast cultures to either obligatory respiratory conditions (containing glycerol as the sole carbon source) or to fermentation and then switched them to the same semifermentative growth conditions. In fact, we observed that wild-type yeast cultures preadapted to respiration demonstrated significantly decreased markers of both oxidative stress and plasma membrane permeabilization as compared with cultures preadapted to fermentation (supplemental Fig. S11). These data demonstrate that also upon our growth conditions increased fermentation is detrimental for cell survival of wild-type cultures.

Next, we sought to evaluate whether enhanced respiratory capacity increases or decreases clonogenic TDP-43-triggered cytotoxicity. We adapted yeast strains transformed with TDP-43-encoding plasmids to respiration by incubating them in obligatory respiratory growth medium (containing glycerol as the sole carbon source) before inducing expression. TDP-43-expressing cultures adapted to fermentation did not show a decrease in clonogenicity at early time points (4–10 h after induction) (Fig. 7*A*). In contrast, at these time points, TDP-43-expressing cultures adapted to respiration exhibited an early and significant decrease in clonogenicity (Fig. 7*A*). Thus, clonogenic cytotoxicity upon TDP-43 expression is markedly accelerated in cultures adapted to respiratory as opposed to fermentative conditions.

Levels of oxidative stress and plasma membrane permeabilization were significantly increased in TDP-43-expressing cultures preadapted to respiration when compared with the vector controls (Fig. 7, *B* and *C*). In contrast, in cultures preadapted to fermentation, the levels of oxidative stress and plasma membrane permeabilization were highly similar between TDP-43-expressing cultures and vector controls (Fig. 7, *B* and *C*). Most notably, the level of morphological markers of apoptotic and necrotic cell death correlated with those of oxidative stress and membrane permeabilization: cell death (both apoptosis and necrosis) was significantly higher in TDP-43-expressing cultures with increased respiratory capacity when compared with cultures adapted to fermentative medium (Fig. 7*D*). Thus, enhanced respiration (and therewith increased electron flux) accelerates and increases TDP-43-triggered cytotoxicity and morphological cell death. TDP-43-triggered cytotoxicity therefore overcompensates for the beneficial role of respiration on cell survival and life span.

To increase the electron flux in the respiratory chain from the starting point of the respiratory chain, we co-expressed TDP-43 with *NDI1*, the gene encoding the internal NADH: ubiquinone oxidoreductase Ndi1p, whose deletion slightly affected clonogenic TDP-43-triggered cytotoxicity (see supplemental Fig. S10). Although we observed no decrease in clonogenicity (data not shown), cultures expressing both *NDI1* and TDP-43 produced significantly more ROS when compared with cells expressing *NDI1* alone (Fig. 7*E*). Notably, although expression of *NDI1* alone was sufficient to reduce oxidative stress levels, this reduction was completely compensated for by co-expression with TDP-43. These data suggest that TDP-43 expression promotes ROS formation upon increased electron flux in the respiratory chain and substantiate our finding that respiration is an important modulator of TDP-43-triggered cytotoxicity and cell death.

DISCUSSION

Yeast Model Providing Insight into TDP-43-triggered Cytotoxicity and Cell Death—We applied a yeast model to dissect cell death mechanisms upon expression of the human neurotoxic protein TDP-43, which plays a pivotal role in the progression of certain ALS and FTLD subtypes. We observed mitochondrion-associated cytoplasmic aggregate-like TDP-43 foci that correlated with cytotoxicity as measured by increased growth defects when spotted onto selective inducing and repressing nutrient-containing solid media. Applying complementary clonogenic and morphological approaches, we conclude that TDP-43-triggered cytotoxicity efficiently results in cell death based on the following observations. (i) TDP-43 expression led to clonogenic cytotoxicity in a dose- and age-dependent manner with an increased phenotype expressing ALS-associated TDP-43-Q331K. (ii) TDP-43-triggered cytotoxicity occurred concomitantly with increased oxidative stress. (iii) TDP-43-triggered cytotoxicity culminated in both apoptotic and necrotic forms of cell death. Previously, complementary biochemical, cell biological, and genetic approaches revealed that TDP-43 expression in yeast results in the formation of cytoplasmic perinuclear

FIGURE 5. **Depleting respiratory chain complexes relieves TDP-43-triggered cytotoxicity.** TDP-43 was expressed from a high copy (2μ) yeast expression plasmid under the control of a *GAL10* promoter in liquid nutrient-containing growth medium with glucose and galactose as in Fig. 4. *Panel 1*, TDP-43 was expressed in wild-type and knock-out strains for 14 h and evaluated for effects on clonogenicity in knock-out strains deleted for integral membrane proteins of the respiratory chain complexes III–V (*A–C*). The mean values of cfus obtained using yeast cells expressing vector controls were set to 100%. Data represent mean values of at least three independent experiments. *Error bars* represent S.E. *p* values were determined with a *t* test by comparing relative clonogenicity of TDP-43-WT in the wild-type strain *versus* knock-out strains. *, $p < 0.05$; **, $p < 0.01$; ***, $p < 0.001$. *Panel 2*, respiratory capacity of the indicated knock-out strains using a clonogenic approach to measure the growth of colonies on solid nutrient-containing growth medium with glycerol as the sole (respiratory) carbon source. The clonogenic respiratory capacity of the wild-type strain was set to 100%. Data represent mean values of three independent experiments except those involving Δ*atp18* for which two experiments were performed. *Error bars* represent S.E. *p* values were determined with a *t* test by comparing clonogenic respiratory capacities of knock-out strains with those of the wild-type strain. *, $p < 0.05$; **, $p < 0.01$; ***, $p < 0.001$. *Panel 3*, correlation of clonogenicity upon TDP-43 expression (see *panel 1*) with clonogenic respiratory capacity of the respective yeast strains (see *panel 2*). The coefficient of determination, R^2, was determined using linear regression (Microsoft Excel 2010). *Panel 4*, mtDNA content in the indicated knock-out strains. The proportion of cells lacking extranuclear mtDNA nucleoids was determined by DAPI staining. Data represent mean values of at least four independent experiments. *Error bars* represent S.E. *p* values were determined with a *t* test by comparing knock-out strains with the wild-type strain. *, $p < 0.05$; **, $p < 0.01$. *Panel 5*, correlation of clonogenicity upon TDP-43 expression (see *panel 1*) with mtDNA content of the respective yeast strains (see *panel 4*). The coefficient of determination, R^2, was determined using logarithmic regression (Microsoft Excel 2010). *ctrl*, control.

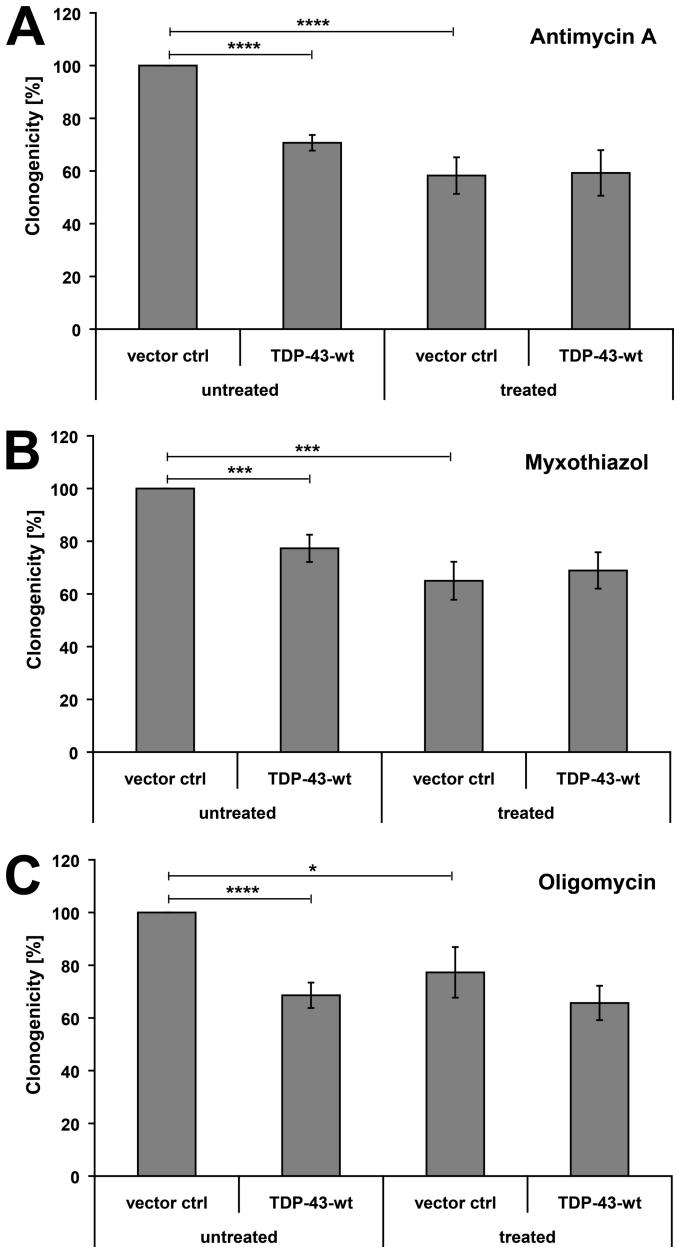

FIGURE 6. **TDP-43-triggered cytotoxicity is not exacerbated by pharmacologically inhibiting respiratory chain complexes.** TDP-43 was expressed from a high copy (2μ) yeast expression plasmid under the control of a *GAL10* promoter in liquid growth medium with glucose and galactose as in Fig. 4. TDP-43 was expressed in the wild-type strain for 15 h in the presence of the respiratory chain inhibitors antimycin A (10 μM) (*A*), myxothiazol (1 μM) (*B*), and oligomycin (1 μg/ml) (*C*) and evaluated for clonogenicity. The mean values of the cfus obtained using untreated yeast cells expressing vector controls were set to 100% in each experiment. Data represent mean values of six independent experiments. *Error bars* represent S.E. *, $p < 0.05$; ***, $p < 0.001$; ****, $p < 0.0001$ (*t* test). *ctrl*, control.

aggregates (13–15). Notably, these aggregates were found to be biochemically distinct from polyglutamine or prion aggregates formed in other neurotoxic yeast models (13). TDP-43 aggregation was dose-dependent and increased in ALS-associated TDP-43 variants, resulting in deleterious growth defects (13–15). We decided to measure cell death (and not growth) with specific assays to reveal clonogenic and morphological cell death and confirmed that TDP-43 expression and aggregation are cytotoxic in yeast. We also demonstrated for the first time that chronological aging exacerbates TDP-43-triggered cytotoxicity and cell death.

Human neurodegenerative disorders with TDP-43 pathologies (*i.e.* ALS and FTLD) are age-dependent diseases with poorly understood mechanisms (1). Mouse, rat, *C. elegans*, and *Drosophila* models overexpressing TDP-43 in neurons display the formation of TDP-43 aggregates and a dose-dependent progressive loss of neurons with morphological features of cell death (3, 6, 8, 51, 52). Similarly, chick embryos and mammalian cell cultures transfected with TDP-43 undergo a time-dependent cell death response (10, 53). Thus, age- and dose-dependent TDP-43 aggregation and TDP-43-triggered cytotoxicity and cell death are common features of various TDP-43 models ranging from animal models to cell cultures and yeast. This underscores the relevance of the yeast model for the genetic and molecular dissection of the cellular mechanisms of TDP-43-triggered cytotoxicity and cell death.

Cell Death Proteases and Mitochondrial Release Factors Are Not Required for TDP-43-triggered Cell Death—Our data demonstrate that deletion of the gene encoding Yca1p, the yeast homolog of mammalian caspases, and deletions of those encoding the other yeast cell death proteases Nma111p, Kex1p, Cpl1p, and Pep4p do not relieve TDP-43-triggered cytotoxicity. In yeast, expression of C-terminal TDP-43 fragments is sufficient to trigger cytotoxicity (13). In mammalian cells, caspase 3-mediated truncation of TDP-43 generates similar C-terminal fragments that are supposed to accelerate cell death; however, these experiments were done under conditions wherein apoptosis and caspase 3 activation were triggered exogenously by pharmacological treatments (4, 7, 10). Although it is unknown whether caspases can be activated intrinsically as a result of aberrant TDP-43 aggregation, our data obtained in yeast suggest that cell death upon TDP-43 expression and aggregation does not require the activation of known cell death proteases.

The findings presented herein also demonstrate that the mitochondrial proteins Aif1p, Nuc1p, and cytochrome *c*, specific mitochondrion-dependent cell death mediators upon their cytosolic release, do not modulate cytotoxicity upon TDP-43 expression. Release of cytochrome *c* into the cytosol and consequent activation of caspases 1 and 3 have been observed during mitochondrion-dependent cell death in mouse and cell culture models of ALS of non-TDP-43-related etiology (54). Also, inhibition of cytochrome *c* release is regarded as a potential therapeutic intervention to delay ALS pathology (54). Despite these findings, our data obtained in yeast suggest that in ALS and FTLD of TDP-43-associated etiology release of cytochrome *c* might be non-essential for cell death, a hypothesis that merits further validation in animal and mammalian cell culture models.

Mitochondrial Respiration Potentiates TDP-43-triggered Cytotoxicity and Cell Death—Our data strongly suggest that respiration and mtDNA content are important factors that modulate TDP-43-triggered cytotoxicity and cell death based on the following findings. (i) Respiration-deficient yeast strains depleted from mtDNA (wild-type ρ^0, Δ*mgm1*, Δ*oxa1*, and Δ*atp4*) were significantly less sensitive to the deleterious effects of TDP-43 expression. (ii) Respiration-deficient knock-out

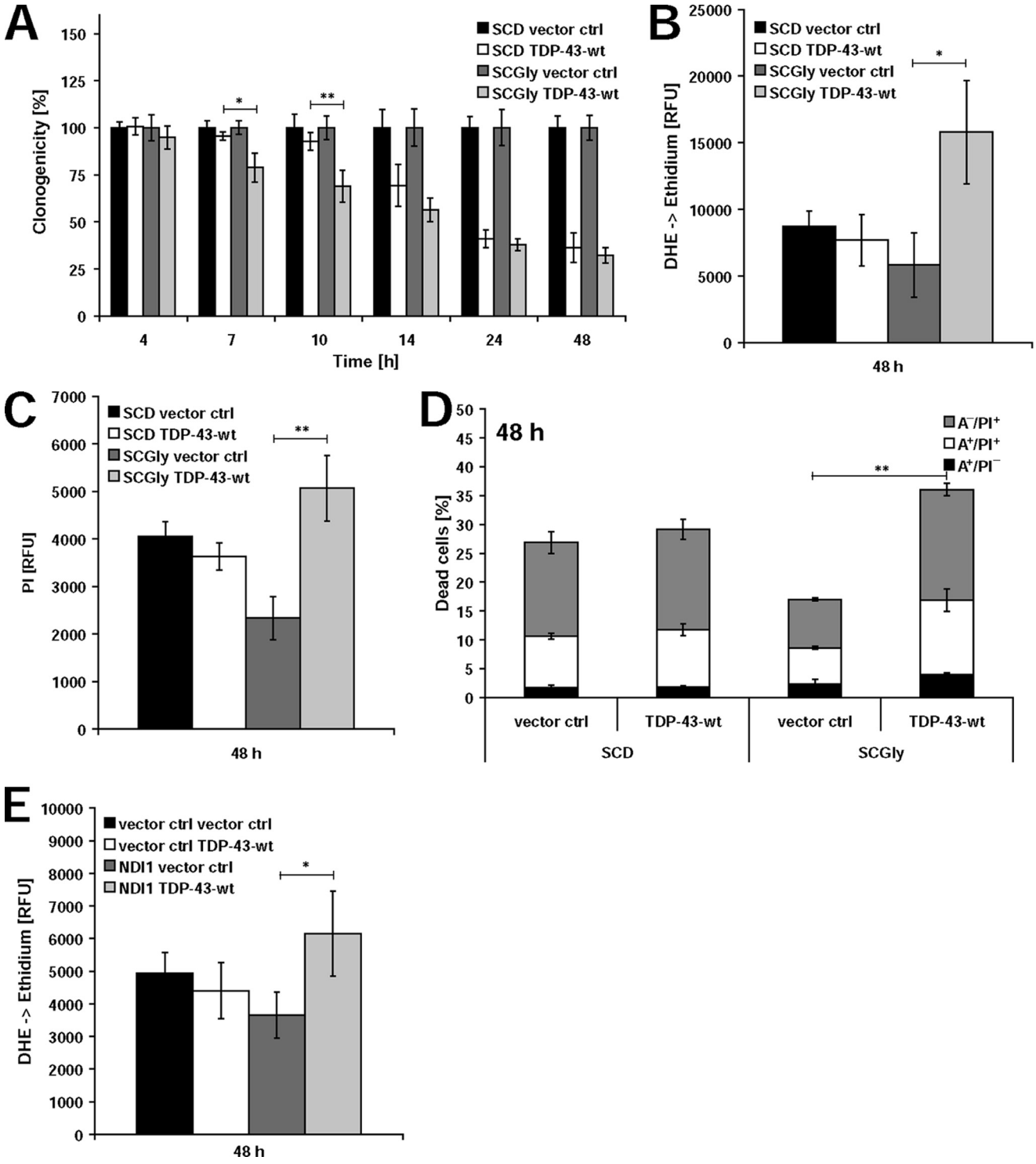

FIGURE 7. **Increased respiratory capacity exacerbates TDP-43-triggered cytotoxicity and cell death.** *A–D*, yeast cells transformed with a high copy (2μ) yeast expression plasmid under the control of a *GAL10* promoter were precultured in either fermentative (glucose) or obligatory respiratory media (glycerol) for 2 days. TDP-43 expression was induced by shifting cells to liquid growth medium containing both glucose and galactose as in Fig. 4. *A*, yeast cells were evaluated for clonogenicity. The mean value of the cfus obtained using yeast cells expressing vector controls was set to 100%. Data represent mean values of at least four independent experiments. *Error bars* represent S.E. *, $p < 0.05$; **, $p < 0.01$ (*t* test). *B* and *C*, oxidative stress levels (DHE staining) and incidences of membrane permeabilization (PI staining) were measured by a fluorescence plate reader at day 2 after inducing TDP-43 expression. Data represent mean values of five independent experiments. *Error bars* represent standard error. *, $p < 0.05$; **, $p < 0.01$ (*t* test, paired). *D*, at 2 days of TDP-43 expression, yeast cells were evaluated quantitatively using FACS analysis to detect morphological markers of cell death. Annexin V $(A)^+$/PI^- and Annexin V^-/PI^+ yeast cells are referred to as (early) apoptotic and necrotic cells, respectively, whereas Annexin V^+/PI^+ yeast cells are referred to as late apoptotic and secondary necrotic cells. Data represent mean values of three experiments performed in parallel. *Error bars* represent S.E. **, $p < 0.01$ (*t* test). *E*, yeast cells were co-transformed with a high copy (2μ) yeast expression plasmid encoding TDP-43 under the control of a *GAL10* promoter and with a low copy (CEN4) yeast expression plasmid encoding *NDI1* under the control of a *GAL1* promoter. TDP-43 and *NDI1* expression was induced by shifting cells to liquid growth medium containing both glucose and galactose as in Fig. 4. Oxidative stress levels (DHE staining) were measured by a fluorescence plate reader 2 days after inducing TDP-43 and *NDI1* expression. Data represent mean values of four independent experiments. *Error bars* represent S.E. *, $p < 0.05$ (*t* test). *ctrl*, control; *RFU*, relative fluorescent units.

strains that retained intact inheritable mtDNA also exhibited significantly decreased TDP-43-triggered cytotoxicity. Notably, the rescuing effect observed with these strains strictly correlated with the extent of respiratory deficiency and the extent of mtDNA instability. (iii) Chemical inhibition of the electron flux through the respiratory chain at the level of complexes III and V did not additionally exacerbate TDP-43-triggered cytotoxicity. (iv) Increasing the electron flux through the respiratory chain by preadapting the strains to obligatory respiratory growth conditions or by causing elevated electron flow through the respiratory chain by overexpressing *NDI1* significantly increased clonogenic and morphological cell death as well as oxidative stress.

Yeast strains that are respiration-deficient due to mtDNA depletion also show relieved cytotoxicity induced by α-synuclein, a major etiological factor in Parkinson disease (47), and by mutant Cdc48p, the yeast ortholog of the human neurotoxic protein valosin-containing protein (39, 55). Albeit our present study was the first systematic analysis that measured the influence of different levels of respiratory capacity on the cytotoxicity of a neurotoxic protein in yeast, these previous studies suggest that mitochondrial respiration might be a more general amplifier of yeast cytotoxicity induced by the expression of neurotoxic proteins.

We observed that wild-type cultures with increased respiratory capacity due to preadaptation to obligatory respiratory medium demonstrated a significantly lower level of morphological cell death as compared with wild-type cultures preadapted to fermentation. These data are in line with previous studies demonstrating that upon chronological aging elevated fermentation increases apoptotic cell death and decreases yeast chronological life span (49). In contrast, respiration is needed in dividing cells for efficient cell killing during seeding and early development of yeast colonies on solid nutrient-containing medium (56). Thus, yeast cell death can either be promoted or decreased by mitochondrial respiration. Upon expression of neurotoxic proteins, such as TDP-43, respiration appears to accelerate age-dependent cell death, presumably overpowering the beneficial effect of respiration on chronological aging of yeast cells.

Neurons obligatorily depend on respiration, exhibiting among the highest respiration rates of all cells (57). Considering this fact, our finding that respiration increases the cytotoxicity of TDP-43 and possibly other human neurotoxic proteins may explain why neurons are particularly vulnerable to the deleterious effects of neurotoxic proteins.

Oxidative Stress and Mitochondrial Dysfunction Are Features of TDP-43-triggered Cytotoxicity—We observed a significant accumulation of ROS upon TDP-43 expression. The levels of oxidative stress were significantly increased upon elevated respiratory capacity, and inactivation of the respiratory chain by genetic intervention significantly decreased TDP-43-triggered cytotoxicity. These data suggest that the mitochondrial respiratory chain is the major origin of the ROS and posit the observed increased and accelerated cytotoxicity of TDP-43 upon increased respiratory capacity to be due to increased ROS production from a disturbed respiratory chain. The pharmacological inactivation of complex III, a known major producer of ROS (58), effectively prevented increased cytotoxicity upon TDP-43 expression, suggesting that this complex specifically contributes to ROS production. We also observed the formation of perimitochondrial foci upon TDP-43 expression in yeast. These data may point to a critical pathological role for TDP-43 aggregates in interfering with the mitochondrial network, culminating in mitochondrial damage and cell death.

The accumulation of ROS and their mitochondrial origin were also described in neurotoxic yeast models expressing α-synuclein (47), disease-associated Huntingtin fragments (59, 60), and mutant Cdc48p, the yeast ortholog of human valosin-containing protein (39, 55). Whereas Huntingtin aggregates were observed to co-migrate and to attach to mitochondria, leading to mitochondrial damage (59, 60), attachment of mutant Cdc48p (39, 55, 61, 62), which does not form aggregates, to mitochondria rather interferes with efficient mitochondrial quality control (61). In contrast, the mechanisms whereby aberrant TDP-43 aggregates interfere with mitochondria will need further experimental analyses.

Oxidative stress and mitochondrial dysfunction are characteristic of nearly all neurodegenerative disorders (63). Accordingly, they are hallmarks of ALS of non-TDP-43-mediated pathology (54), and studies in animal and cell culture models have indicated that abnormal mitochondrial morphology and bioenergetics are crucially involved in the pathogenicity underlying the major subtype of familial ALS caused by mutations of superoxide dismutase 1 (SOD1) (54). Additionally, in mouse models of FTLD caused by mutations in the microtubule-associated protein tau, mitochondrial dysfunction strongly correlates with decreased respiratory activity (64, 65). Because TDP-43-associated pathology is a characteristic feature of subtypes of both ALS and FTLD (1), it is likely that mitochondria also play a role in these subtypes of diseases as well. Indeed, very recent data demonstrated a decrease in mitochondrial membrane potential in a neuronal cell culture upon ectopic expression of TDP-43 (44), and abnormal mitochondrial aggregation was observed in primary neurons from a transgenic TDP-43 mouse model (45, 46). Our data therefore substantiate these recent studies and strongly suggest that oxidative stress and mitochondrial dysfunction are important in triggering cell death in TDP-43-triggered ALS and FTLD. Furthermore, we demonstrated that respiratory capacity is a major determinant of TDP-43-triggered cytotoxicity.

Comparing yeast models for TDP-43 proteinopathies and for other neurodegenerative disorders may be an ideal context to identify specific and common modulators of critical mitochondrial dysfunction and to reveal the role of cellular metabolism on neurotoxic cell death scenarios. Specifically in yeast, in marked contrast to mammalian cell cultures, the respiratory state can easily be modified by switching from fermentative to semifermentative and obligatory respiratory metabolism simply by changing the carbon source. Despite the fact that yeast cells are not neurons and therefore their energy utilization might be different from that of neurons, this will facilitate the targeted validation of the identified mechanisms in higher systems that do have a nervous system.

Acknowledgments—We are grateful to Prof. Dr. Benedikt Westermann for helpful comments and critical reading of the manuscript, and Dr. Eric Hummel for support with fluorescence microscopy, Prof. Dr. Aaron Gitler for providing reagents.

REFERENCES

1. Neumann, M. (2009) *Int. J. Mol. Sci.* **10,** 232–246
2. Wang, I. F., Wu, L. S., and Shen, C. K. (2008) *Trends Mol. Med.* **14,** 479–485
3. Ash, P. E., Zhang, Y. J., Roberts, C. M., Saldi, T., Hutter, H., Buratti, E., Petrucelli, L., and Link, C. D. (2010) *Hum. Mol. Genet* **19,** 3206–3218
4. Dormann, D., Capell, A., Carlson, A. M., Shankaran, S. S., Rodde, R., Neumann, M., Kremmer, E., Matsuwaki, T., Yamanouchi, K., Nishihara, M., and Haass, C. (2009) *J. Neurochem.* **110,** 1082–1094
5. Fiesel, F. C., Voigt, A., Weber, S. S., Van den Haute, C., Waldenmaier, A., Görner, K., Walter, M., Anderson, M. L., Kern, J. V., Rasse, T. M., Schmidt, T., Springer, W., Kirchner, R., Bonin, M., Neumann, M., Baekelandt, V., Alunni-Fabbroni, M., Schulz, J. B., and Kahle, P. J. (2010) *EMBO J.* **29,** 209–221
6. Hanson, K. A., Kim, S. H., Wassarman, D. A., and Tibbetts, R. S. (2010) *J. Biol. Chem.* **285,** 11068–11072
7. Igaz, L. M., Kwong, L. K., Chen-Plotkin, A., Winton, M. J., Unger, T. L., Xu, Y., Neumann, M., Trojanowski, J. Q., and Lee, V. M. (2009) *J. Biol. Chem.* **284,** 8516–8524
8. Wegorzewska, I., Bell, S., Cairns, N. J., Miller, T. M., and Baloh, R. H. (2009) *Proc. Natl. Acad. Sci. U.S.A.* **106,** 18809–18814
9. Wils, H., Kleinberger, G., Janssens, J., Pereson, S., Joris, G., Cuijt, I., Smits, V., Ceuterick-de Groote, C., Van Broeckhoven, C., and Kumar-Singh, S. (2010) *Proc. Natl. Acad. Sci. U.S.A.* **107,** 3858–3863
10. Zhang, Y. J., Xu, Y. F., Cook, C., Gendron, T. F., Roettges, P., Link, C. D., Lin, W. L., Tong, J., Castanedes-Casey, M., Ash, P., Gass, J., Rangachari, V., Buratti, E., Baralle, F., Golde, T. E., Dickson, D. W., and Petrucelli, L. (2009) *Proc. Natl. Acad. Sci. U.S.A.* **106,** 7607–7612
11. Zhou, H., Huang, C., Chen, H., Wang, D., Landel, C. P., Xia, P. Y., Bowser, R., Liu, Y. J., and Xia, X. G. (2010) *PLoS Genet.* **6,** e1000887
12. Li, Y., Ray, P., Rao, E. J., Shi, C., Guo, W., Chen, X., Woodruff, E. A., 3rd, Fushimi, K., and Wu, J. Y. (2010) *Proc. Natl. Acad. Sci. U.S.A.* **107,** 3169–3174
13. Johnson, B. S., McCaffery, J. M., Lindquist, S., and Gitler, A. D. (2008) *Proc. Natl. Acad. Sci. U.S.A.* **105,** 6439–6444
14. Johnson, B. S., Snead, D., Lee, J. J., McCaffery, J. M., Shorter, J., and Gitler, A. D. (2009) *J. Biol. Chem.* **284,** 20329–20339
15. Armakola, M., Hart, M. P., and Gitler, A. D. (2011) *Methods* **53,** 238–245
16. Eisenberg, T., Büttner, S., Kroemer, G., and Madeo, F. (2007) *Apoptosis* **12,** 1011–1023
17. Madeo, F., Carmona-Gutierrez, D., Ring, J., Büttner, S., Eisenberg, T., and Kroemer, G. (2009) *Biochem. Biophys. Res. Commun.* **382,** 227–231
18. Carmona-Gutierrez, D., Eisenberg, T., Büttner, S., Meisinger, C., Kroemer, G., and Madeo, F. (2010) *Cell Death Differ.* **17,** 763–773
19. Eisenberg, T., Knauer, H., Schauer, A., Büttner, S., Ruckenstuhl, C., Carmona-Gutierrez, D., Ring, J., Schroeder, S., Magnes, C., Antonacci, L., Fussi, H., Deszcz, L., Hartl, R., Schraml, E., Criollo, A., Megalou, E., Weiskopf, D., Laun, P., Heeren, G., Breitenbach, M., Grubeck-Loebenstein, B., Herker, E., Fahrenkrog, B., Fröhlich, K. U., Sinner, F., Tavernarakis, N., Minois, N., Kroemer, G., and Madeo, F. (2009) *Nat. Cell Biol.* **11,** 1305–1314
20. Madeo, F., Fröhlich, E., and Fröhlich, K. U. (1997) *J. Cell Biol.* **139,** 729–734
21. Eisenberg, T., Carmona-Gutierrez, D., Büttner, S., Tavernarakis, N., and Madeo, F. (2010) *Apoptosis* **15,** 257–268
22. Mason, D. A., Shulga, N., Undavai, S., Ferrando-May, E., Rexach, M. F., and Goldfarb, D. S. (2005) *FEMS Yeast Res.* **5,** 1237–1251
23. Madeo, F., Herker, E., Maldener, C., Wissing, S., Lächelt, S., Herlan, M., Fehr, M., Lauber, K., Sigrist, S. J., Wesselborg, S., and Fröhlich, K. U. (2002) *Mol. Cell* **9,** 911–917
24. Hauptmann, P., and Lehle, L. (2008) *J. Biol. Chem.* **283,** 19151–19163
25. Fahrenkrog, B., Sauder, U., and Aebi, U. (2004) *J. Cell Sci.* **117,** 115–126
26. Hayashi, M., Fukuzawa, T., Sorimachi, H., and Maeda, T. (2005) *Mol. Cell. Biol.* **25,** 9478–9490
27. Carmona-Gutierrez, D., Fröhlich, K. U., Kroemer, G., and Madeo, F. (2010) *Cell Death Differ.* **17,** 377–378
28. Büttner, S., Eisenberg, T., Carmona-Gutierrez, D., Ruli, D., Knauer, H., Ruckenstuhl, C., Sigrist, C., Wissing, S., Kollroser, M., Fröhlich, K. U., Sigrist, S., and Madeo, F. (2007) *Mol. Cell* **25,** 233–246
29. Wissing, S., Ludovico, P., Herker, E., Büttner, S., Engelhardt, S. M., Decker, T., Link, A., Proksch, A., Rodrigues, F., Corte-Real, M., Fröhlich, K. U., Manns, J., Candé, C., Sigrist, S. J., Kroemer, G., and Madeo, F. (2004) *J. Cell Biol.* **166,** 969–974
30. Li, W., Sun, L., Liang, Q., Wang, J., Mo, W., and Zhou, B. (2006) *Mol. Biol. Cell* **17,** 1802–1811
31. Herker, E., Jungwirth, H., Lehmann, K. A., Maldener, C., Fröhlich, K. U., Wissing, S., Büttner, S., Fehr, M., Sigrist, S., and Madeo, F. (2004) *J. Cell Biol.* **164,** 501–507
32. Madeo, F., Fröhlich, E., Ligr, M., Grey, M., Sigrist, S. J., Wolf, D. H., and Fröhlich, K. U. (1999) *J. Cell Biol.* **145,** 757–767
33. Braun, R. J., Büttner, S., Ring, J., Kroemer, G., and Madeo, F. (2010) *Trends Biochem. Sci.* **35,** 135–144
34. Gitler, A. D. (2008) *Neurosignals* **16,** 52–62
35. Outeiro, T. F., and Giorgini, F. (2006) *Biotechnol. J.* **1,** 258–269
36. Khurana, V., and Lindquist, S. (2010) *Nat. Rev. Neurosci.* **11,** 436–449
37. Westermann, B., and Neupert, W. (2000) *Yeast* **16,** 1421–1427
38. Merz, S., and Westermann, B. (2009) *Genome Biol.* **10,** R95
39. Braun, R. J., Zischka, H., Madeo, F., Eisenberg, T., Wissing, S., Büttner, S., Engelhardt, S. M., Büringer, D., and Ueffing, M. (2006) *J. Biol. Chem.* **281,** 25757–25767
40. Kushnirov, V. V. (2000) *Yeast* **16,** 857–860
41. Towbin, H., Staehelin, T., and Gordon, J. (1979) *Proc. Natl. Acad. Sci. U.S.A.* **76,** 4350–4354
42. Laemmli, U. K. (1970) *Nature* **227,** 680–685
43. Martin, L. J. (2010) *Pharmaceuticals* **3,** 839–915
44. Duan, W., Li, X., Shi, J., Guo, Y., Li, Z., and Li, C. (2010) *Neuroscience* **169,** 1621–1629
45. Xu, Y. F., Gendron, T. F., Zhang, Y. J., Lin, W. L., D'Alton, S., Sheng, H., Casey, M. C., Tong, J., Knight, J., Yu, X., Rademakers, R., Boylan, K., Hutton, M., McGowan, E., Dickson, D. W., Lewis, J., and Petrucelli, L. (2010) *J. Neurosci.* **30,** 10851–10859
46. Shan, X., Chiang, P. M., Price, D. L., and Wong, P. C. (2010) *Proc. Natl. Acad. Sci. U.S.A.* **107,** 16325–16330
47. Büttner, S., Bitto, A., Ring, J., Augsten, M., Zabrocki, P., Eisenberg, T., Jungwirth, H., Hutter, S., Carmona-Gutierrez, D., Kroemer, G., Winderickx, J., and Madeo, F. (2008) *J. Biol. Chem.* **283,** 7554–7560
48. Ludovico, P., Rodrigues, F., Almeida, A., Silva, M. T., Barrientos, A., and Côrte-Real, M. (2002) *Mol. Biol. Cell* **13,** 2598–2606
49. Ruckenstuhl, C., Carmona-Gutierrez, D., and Madeo, F. (2010) *Aging* **2,** 643–649
50. Wei, M., Fabrizio, P., Madia, F., Hu, J., Ge, H., Li, L. M., and Longo, V. D. (2009) *PLoS Genet.* **5,** e1000467
51. Tatom, J. B., Wang, D. B., Dayton, R. D., Skalli, O., Hutton, M. L., Dickson, D. W., and Klein, R. L. (2009) *Mol. Ther.* **17,** 607–613
52. Ritson, G. P., Custer, S. K., Freibaum, B. D., Guinto, J. B., Geffel, D., Moore, J., Tang, W., Winton, M. J., Neumann, M., Trojanowski, J. Q., Lee, V. M., Forman, M. S., and Taylor, J. P. (2010) *J. Neurosci.* **30,** 7729–7739
53. Sreedharan, J., Blair, I. P., Tripathi, V. B., Hu, X., Vance, C., Rogelj, B., Ackerley, S., Durnall, J. C., Williams, K. L., Buratti, E., Baralle, F., de Belleroche, J., Mitchell, J. D., Leigh, P. N., Al-Chalabi, A., Miller, C. C., Nicholson, G., and Shaw, C. E. (2008) *Science* **319,** 1668–1672
54. Shi, P., Gal, J., Kwinter, D. M., Liu, X., and Zhu, H. (2010) *Biochim. Biophys. Acta* **1802,** 45–51
55. Braun, R. J., and Zischka, H. (2008) *Biochim. Biophys. Acta* **1783,** 1418–1435
56. Ruckenstuhl, C., Büttner, S., Carmona-Gutierrez, D., Eisenberg, T., Kroemer, G., Sigrist, S. J., Fröhlich, K. U., and Madeo, F. (2009) *PLoS One* **4,** e4592
57. Bolaños, J. P., Almeida, A., and Moncada, S. (2010) *Trends Biochem. Sci.*

35, 145–149
58. Fang, J., and Beattie, D. S. (2003) *Free Radic. Biol. Med.* **34,** 478–488
59. Ocampo, A., Zambrano, A., and Barrientos, A. (2010) *FASEB J.* **24,** 1431–1441
60. Solans, A., Zambrano, A., Rodríguez, M., and Barrientos, A. (2006) *Hum. Mol. Genet.* **15,** 3063–3081
61. Heo, J. M., Livnat-Levanon, N., Taylor, E. B., Jones, K. T., Dephoure, N., Ring, J., Xie, J., Brodsky, J. L., Madeo, F., Gygi, S. P., Ashrafi, K., Glickman, M. H., and Rutter, J. (2010) *Mol. Cell* **40,** 465–480
62. Zischka, H., Braun, R. J., Marantidis, E. P., Büringer, D., Bornhövd, C., Hauck, S. M., Demmer, O., Gloeckner, C. J., Reichert, A. S., Madeo, F., and Ueffing, M. (2006) *Mol. Cell. Proteomics* **5,** 2185–2200
63. Fukui, H., and Moraes, C. T. (2008) *Trends Neurosci.* **31,** 251–256
64. Eckert, A., Hauptmann, S., Scherping, I., Meinhardt, J., Rhein, V., Dröse, S., Brandt, U., Fändrich, M., Müller, W. E., and Götz, J. (2008) *J. Mol. Med.* **86,** 1255–1267
65. Deters, N., Ittner, L. M., and Götz, J. (2008) *Eur. J. Neurosci.* **28,** 137–147